J Nanopart Res (2016) 18: 327
DOI 10.1007/s11051-016-3630-8

RESEARCH PAPER

Colorimetric detection of Cd^{2+} using 1-amino-2-naphthol-4-sulfonic acid functionalized silver nanoparticles

Pengcheng Huang · Bowen Liu · Weiwei Jin · Fangying Wu · Yiqun Wan

Received: 16 June 2016 / Accepted: 15 October 2016 / Published online: 9 November 2016

Abstract A colorimetric assay has been developed for facile, rapid, and sensitive detection of Cd^{2+} using 1-amino-2-naphthol-4-sulfonic acid functionalized silver nanoparticles (ANS-AgNPs). The presence of Cd^{2+} induces the aggregation of ANS-AgNPs through cooperative metal–ligand interaction. As a result, the characteristic surface plasmon resonance (SPR) peak of ANS-AgNPs at 390 nm was red-shifted to 580 nm, yielding a color change from bright yellow to reddish-brown. The color change is monitored by UV–Vis spectrometer and can be directly read out by the naked eye. Under the optimized conditions, a good linear relationship (correlation coefficient $R = 0.997$) was obtained between the ratio of the absorbance at 580 nm to that at 390 nm (A_{580nm}/A_{390nm}) and the concentration of Cd^{2+} over the range of 1.0–10 μM with detection limit of 87 nM. The proposed method is simple and efficient, which has been applied for determining Cd^{2+} in milk powder, serum, and lake water with satisfactory results.

Keywords Silver nanoparticles · 1-Amino-2-naphthol-4-sulfonic acid · Colorimetric assay · Cd^{2+} · Sensors · Colloids

Electronic supplementary material The online version of this article (doi:10.1007/s11051-016-3630-8) contains supplementary material, which is available to authorized users.

P. Huang · B. Liu · W. Jin · F. Wu (✉) · Y. Wan
College of Chemistry, Nanchang University, Nanchang 330031, China
e-mail: fywu@ncu.edu.cn

Introduction

Nowadays, the pollution caused by heavy metals in nature is a great concern due to potentially toxic effects on living creatures. Cadmium, a nonessential element for life, is widely used in fertilizers, pesticides, nickel-cadmium batteries, dyes, pigments, and coating of steel and various alloys, resulting in the widespread contamination of it in air, soil, and water (Dobson 1992; McLaughlin and Singh 1999). Cadmium has been recognized as a highly toxic heavy metal ion and is enlisted by the US Environmental Protection Agency, Disease Registry, and Agency for toxic substances as one of the superior pollutants. It accumulates in the human body with a long biological half-life of two to three decades. As a consequence of the food chain system, cadmium exposure can cause anemia, abdominal pain, neurological and adverse developmental effects, kidney damage, hypertension, and changes in vitamin D metabolism (Daher 1995; Darwish and Blake 2001; Davis et al. 2006; Friberg et al. 1992; Martinez and Blasco 2012). In addition, chronic exposure to Cd^{2+} has implicated a cause of cancer in lungs, prostate, pancreas, and kidney and even increased risk of cancer (Akesson et al. 2008; Jane et al. 2006). Therefore, the accurate determination of Cd^{2+} is critical.

Scientists have been dedicated to developing the facile detection of Cd^{2+} for the purpose of public health. The techniques currently available for the detection of Cd^{2+} include flame atomic absorption spectrometry (Mirabi et al. 2015), electrochemical analysis (Willemse et al. 2011), inductively coupled plasma

atomic emission spectrometry (Matsumoto et al. 2010), atomic fluorescence spectrometry (Wan et al. 2006), inductively coupled plasma mass spectrometry (Guo et al. 2010), and molecular fluorescence spectroscopy (Yunus et al. 2008). Although these methods offer excellent sensitivity and multielement analysis, they are expensive, time-consuming, intricate, and arduous for on-site field analysis. Hence, the interest in swapping instrumental analytical tools with suitable, selective, sensitive, and low-cost Cd^{2+} sensors has been increasing.

To date, optical sensors, especially the colorimetric ones, have always been the most convenient analytical tool and gained a lot of interest because they provide a simple and economical assay without the aid of expensive instruments (Chansuvarn et al. 2015; Ratnarathron et al. 2015; Zhan et al. 2015). Compared with the well-developed chromophoric chemosensors, metal nanoparticle-based colorimetric assays have recently emerged as a fascinating research field (Chen et al. 2015a, 2015b; Mehta et al. 2015; Sharif et al. 2015; Yang et al. 2014). Among them, gold and silver nanoparticles (AuNPs, AgNPs) are of particular interest as they have played significant roles in environmental monitoring and biological sensing (Chen et al. 2015a, 2015b; Medley et al. 2008). One feature that makes them particularly outstanding is that AuNPs and AgNPs possess high extinction coefficients in the visible region. The colors of the dispersed and aggregated nanoparticle solution are different. For example, the dispersed AgNP solution is bright yellow, while the highly aggregated AgNP solution is red or blue (Zhang and Ye 2011). Many metal nanoparticles have been recently used for the determination of Cd^{2+}. For example, Zhang's group (Zhang et al. 2012) developed a peptide-modified AuNP-based colorimetric method for the parallel detection of Cd^{2+}, Ni^{2+}, and Co^{2+} in river water. Guo et al. (2014) reported a novel method for Cd^{2+} based on label-free AuNPs with the aid of high salt concentration and glutathione. Most recently, Manjumeena et al. (2015) also developed a glutathione functionalized green AuNP probe for the precise colorimetric detection of Cd^{2+} contamination in the environment. Kumar and Anthony (2014) reported a selective colorimetric sensor for Cd^{2+}, Hg^{2+}, and Pb^{2+} ions using costabilizing agents. Obviously, the distinctive properties of AuNPs/AgNPs make them very useful for the development of colorimetric sensing for Cd^{2+}, but it is still demanding to develop novel colorimetric methods to detect Cd^{2+} with better sensitivity and selectivity.

Herein, we report a simple, rapid, selective, and sensitive colorimetric method for the detection of Cd^{2+} in various real samples using 1-amino-2-naphthol-4-sulfonic acid (ANS)-AgNPs as a probe. This sensing strategy is based on the aggregation of ANS-AgNPs induced by Cd^{2+}, which resulted in a red shift in the surface plasmon resonance (SPR) absorption band and an appreciable color change from bright yellow to reddish-brown. The bare AgNPs were functionalized with ANS and used as sensors for the colorimetric detection of Cd^{2+} by taking advantage of metal chelation of Cd^{2+} with the hydroxyl group (–OH) and amino group (–NH_2) of ANS on the surface of AgNPs (Scheme 1).

Materials and methods

Chemicals and materials

All chemicals used were of analytical grade or of the highest purity available. Silver nitrate, sodium borohydride, ANS, and metal salts were purchased from Shanghai Qingxi Technology Co., Ltd. (Shanghai, China, www.ce-r.cn/sites/qingxi/). All glassware was cleaned thoroughly with freshly prepared aqua regia (3:1 (*v*/*v*) HCl/HNO_3) and rinsed thoroughly with doubly distilled water prior to use. Doubly distilled water was used to prepare all the solutions in this study.

Instruments

UV–Vis absorption spectra were examined on a UV-2550 spectrophotometer (Shimadzu, Kyoto, Japan) using a 1.0-cm quartz cell at room temperature. The infrared spectra were measured in KBr pellets with a Nicolet 5700 FTIR Spectrum (Nicolet, USA). Transmission electron micrograph (TEM) was recorded by a JEM-2100 transmission electron microscope (JEOL Ltd., Japan). The data of dynamic light scattering (DLS) were obtained on an NPA152 nanoparticle size analyzer (Microtrac Inc., USA). Photographs were taken with Sony DSC-TX5 camera (Tokyo, Japan).

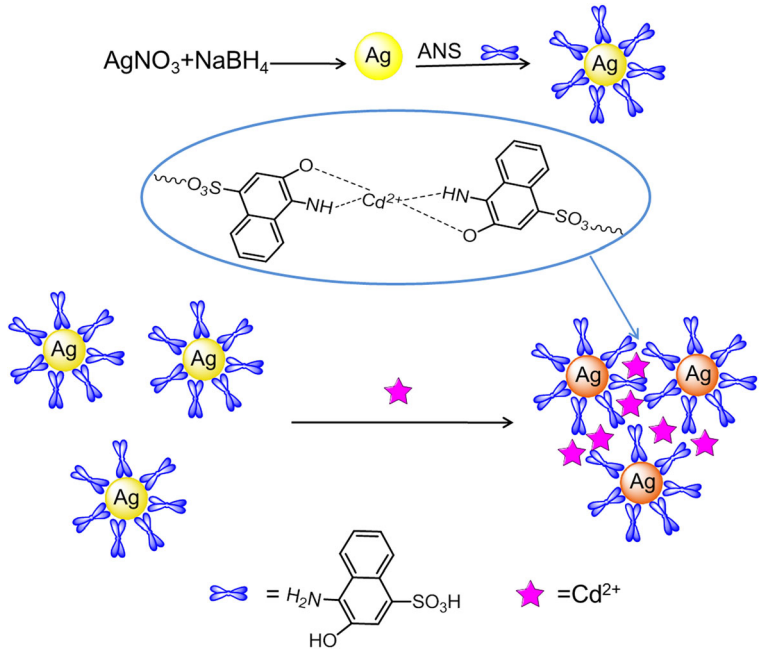

Scheme 1 Schematic representation for the detection of Cd^{2+} by ANS-modified AgNPs

Surface modification of AgNPs or AuNPs with ANS

AgNPs were prepared by the reduction of $AgNO_3$ with $NaBH_4$ according to a previously reported method (Li et al. 2010). Briefly, in a flask, 2.0 mL of 0.01 M $AgNO_3$ was added into 97.5 mL doubly distilled water. Then, 8.8 mg of $NaBH_4$ was quickly added into the above mixture solution under vigorous stirring for 30 min at room temperature (25 ± 2 °C). To obtain ANS-AgNPs, 0.5 mL of 0.01 M ANS was added into the above aqueous solution and then stirred for 2 h at room temperature to functionalize the surface of AgNPs with ANS. Finally, the as-prepared silver colloidal solution was stored at 4 °C in the dark before use.

Citrate-capped AuNPs were prepared by means of the chemical reduction of $HAuCl_4$ as follows. A one hundred-milliliter aqueous solution of 1.0 mM $HAuCl_4$ was brought to a boil with vigorous stirring in a round-bottom flask fitted with a reflux condenser. Trisodium citrate (38.8 mM, 10 mL) was then added rapidly to the solution, and the mixture was heated under reflux for another 15 min. The solution was cooled to room temperature while being stirred continuously. The obtained wine-red solution was stored at 4 °C for further use. For surface modification of AuNPs with ANS, 0.5 mL of 0.01 M ANS was added into the above aqueous solution. The resulted mixture was equilibrated at room temperature for 2 h. Finally, the as-prepared silver colloidal solution was stored at 4 °C in the dark before use.

Colorimetric detection of Cd^{2+}

The following procedure was used for colorimetric detection of Cd^{2+} using ANS-AgNPs as a probe. Briefly, different concentrations of Cd^{2+} solutions were added into the 2.0-mL ANS-AgNP solution. The mixed solution was vortexed for 30 s and then allowed to stand for 5 min at room temperature. Absorption spectra were recorded accordingly. The magnitude of absorbance ratio (A_{580nm}/A_{390nm}) has been used as the index parameter for Cd^{2+} detection, and the numerator and the denominator represent the degree of aggregation and dispersion, respectively.

Results and discussion

Characterization of ANS modified AgNPs

The formation of ANS-AgNPs is estimated by the color change of the solution and further confirmed by the FT-IR spectra of ANS and ANS-AgNPs. It could be observed that the color of the reaction solution turned bright yellow from colorless. Figure S1 displays FT-IR

spectra of ANS and ANS-AgNPs. It was noteworthy that the bands in the range of 900–650 cm^{-1} which are the out-of-plane bending vibration band of the amino group and the band at about 3230 cm^{-1} corresponding to –NH asymmetric stretching vibrations appeared in the spectra of both ANS and ANS-AgNPs, although the peak slightly shifted. It was also found that the wave number at 1350 cm^{-1} is the bending vibration band of –OH located in the spectra of both ANS and ANS-AgNPs. For pure ANS, the peaks at 1162 and 1200 cm^{-1} are assigned to the characteristic stretching vibration absorption of the $–SO_3H$ group, which were hardly to be seen in the spectrum of ANS-AgNPs, indicating that ANS had been successfully bound onto the surface of the AgNPs via the sulfonic group of ANS. Besides, from the TEM image of ANS-AgNPs in Fig. S2, it was found that a dark core was surrounded by a light shell for the AgNPs, and the corresponding high-resolution TEM (HRTEM) image showed that the core had the lattice fringe with interplanar spacings of 0.235 nm ascribed to the (111) plane of Ag, indicating the successful modification of ANS as the ligand on the AgNP surface. In addition, in Fig. S3, for the ANS-AgNPs, the full-scale XPS spectrum showed the characteristic peaks of C 1s, N 1s, O 1s, S 2p, and Ag 3d, further suggesting that ANS was successfully anchored on the AgNP surface. It should be noted that the peaks of the N and S elements were relatively weak, which was possibly because their contents were very low compared with other elements like C and O in ANS. These results revealed that ANS molecules were successfully attached onto the surface of the AgNPs.

To evaluate surface capacity of the ANS on the AgNPs, we compared the fluorescence intensities at ca. 440 nm of supernatant solution of ANS-AgNPs and pure ANS solution before functionalization (Fig. S4). It was found that approximately 54 % of ANS was bound onto the AuNPs, from which we can calculate the amount of ligands to be about 1931 ANS molecules per AgNP.

Selective response of ANS-AgNPs to Cd^{2+}

When the ANS-AgNPs are well dispersed in solution, the colloids exhibit a characteristic SPR band at 390 nm in the UV–Vis absorption spectrum and a bright yellow color. However, upon addition of Cd^{2+}, the absorbance at 390 nm decreased sharply, along with the emergence of a long wavelength band at ca. 580 nm (Fig. 1a). Meanwhile, the color of the ANS-AgNPs immediately changed from yellow to reddish-brown, as depicted in Fig. 1b. Both the spectral and color changes indicated the aggregation of AgNPs induced by Cd^{2+}, which will also be demonstrated below.

In order to investigate the recognition ability of ANS-AgNPs toward metal ions, the specificity of this method was also evaluated with other metal ions (Cu^{2+}, Co^{2+}, Ni^{2+}, Hg^{2+}, Fe^{3+}, Al^{3+}, Cr^{3+}, Ba^{2+}, Pb^{2+}, Ca^{2+}, Mg^{2+}, Zn^{2+}, Mn^{2+}, and Ag^{+}). The study revealed that the spectrum of ANS-AgNPs had little change in the presence of almost common metal ions. As Ni^{2+}, Co^{2+}, and Pb^{2+} had a slight effect on the spectrum of ANS-AgNPs, methylimidazole was applied as the masking agent. The result showed that after masking, Ni^{2+}, Co^{2+}, and Pb^{2+} did not affect the detection of Cd^{2+} (Fig. S5). It should be noted that although methylimidazole was introduced, the spectra were pretty much the same as that of pure ANS-AgNPs for other metal ions and that the response to Cd^{2+} was not influenced, either. This was directly evidenced from Fig. 1b, in which all colorimetric tubes demonstrate bright yellow color after the masking except that Cd^{2+} induced the color change of ANS-AgNPs. So, the developed strategy was highly selective toward Cd^{2+}.

Mechanism of the sensing system

The spectral and color changes of ANS-AgNPs upon addition of Cd^{2+} could be well explained by the aggregation of ANS-AgNPs through the coordination interaction between Cd^{2+} and ANS. ANS-AgNPs were stabilized in solution because ANS on the surface of AgNPs protected them from aggregation. ANS has $–NH_2$, $–SO_3$, and –OH groups, which can be used to bind with metal ions (Jaliehvand et al. 2009; Xue et al. 2011). As shown in Scheme 1, ANS is linked with AgNPs through $–SO_3H$, and owing to the interactions between the O atom in the –OH group and the N atom in the $–NH_2$ group of ANS and Cd^{2+}, the neighboring AgNPs became closer and finally aggregated.

DLS analysis (Fig. 2a) clearly exhibited that Cd^{2+} can cause the aggregation of ANS-AgNPs. The intensity contribution versus diameters of ANS-AgNPs in the absence and presence of Cd^{2+}, around 12 and 28 nm, respectively, also suggested that Cd^{2+} could result in the effective aggregation of ANS-AgNPs. Furthermore, the TEM images revealed monodispersed ANS-AgNPs in the absence of Cd^{2+} and a significant aggregation in the

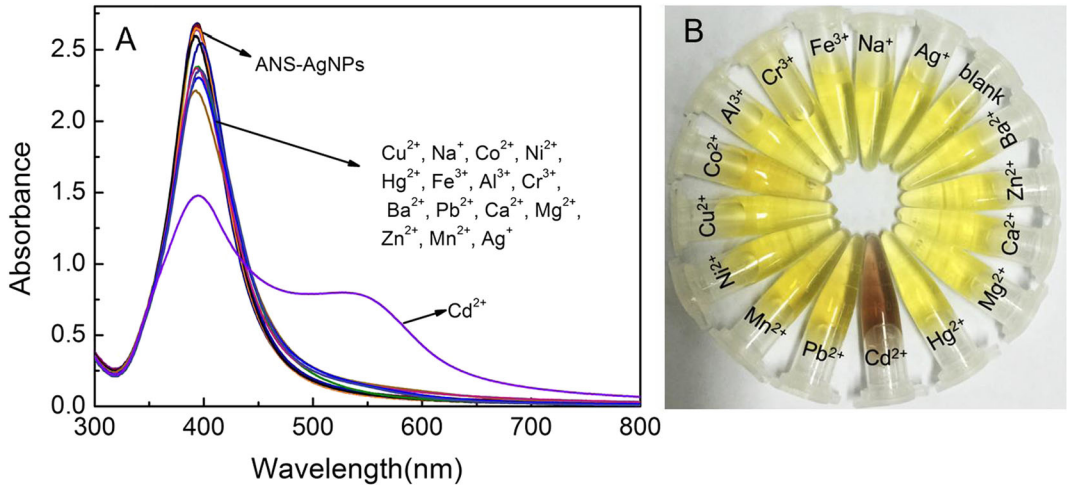

Fig. 1 **a** UV-visible absorption spectra and **b** a photograph of ANS-AgNPs in the presence of different metal ions (Cu^{2+}, Cd^{2+}, Co^{2+}, Ni^{2+}, Hg^{2+}, Fe^{3+}, Al^{3+}, Cr^{3+}, Ba^{2+}, Pb^{2+}, Ca^{2+}, Mg^{2+}, Zn^{2+}, Mn^{2+}, and Ag^{+}; the concentrations of metal ions are all 5.0 μM)

presence of Cd^{2+}, as seen in Fig. 2b. The as-prepared ANS-AgNPs tended to aggregate due to the strong coordination bond between Cd^{2+} and ANS, which could be easily confirmed by the addition of powerful chelating agent ethylenediaminetetraacetic acid (EDTA). The presence of EDTA recovered the absorption spectrum of ANS-AgNPs almost to the original state (Fig. S6).

Optimization of the sensing conditions

Effect of ANS concentration

Parameter ascertainment and optimization of the present method are key factors to its performance in terms of effectiveness and sensitivity, which strongly depends on

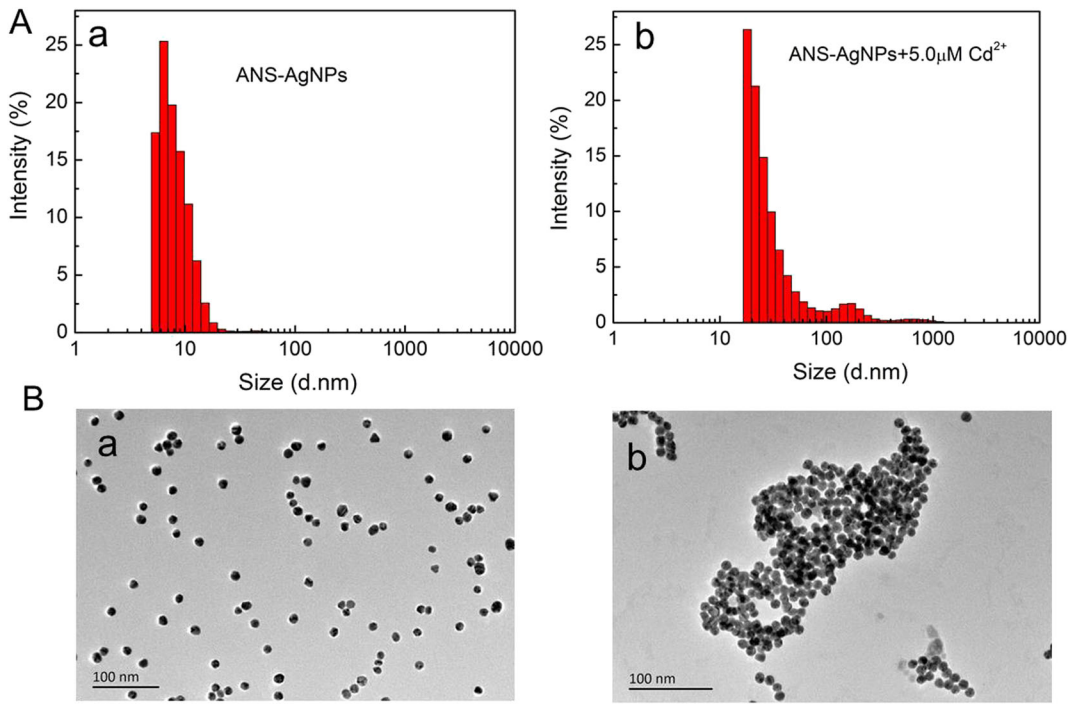

Fig. 2 Size distribution (**a**) and TEM images (**b**) of the ANS-AgNPs in the absence (*a*) and presence of 5.0 μM Cd^{2+} (*b*)

the ANS concentration. Since the concentration of ANS could have an effect on ANS-AgNP detection capability, the stoichiometric ratios between ANS and AgNPs were explored. In our work, it was found that the absorbance ratio (A_{580nm}/A_{390nm}) increased with various molar ratios of AgNPs and ANS (2:1, 4:1, 8:1). As seen in Fig. 3, the lower the molar ratio of AgNPs and ANS was, the worse the capability of Cd^{2+} detection was. In contrast, when the molar ratio of AgNPs and ANS was higher than 4:1, the response of Cd^{2+} to ANS-AgNPs became worse. Based on above results, the molar ratio of 4:1 between AgNPs and ANS was considered to be optimal for Cd^{2+} detection.

Effect of pH and reaction time

The effect of pH on the interaction between ANS-AgNPs and Cd^{2+} was studied over the pH range from 4.0 to 12 (Fig. S7A). When the pH value was less than 4.0, ANS-AgNPs were unstable and aggregated easily. High pH value more than 12 is not beneficial since Cd^{2+} may react with OH^- to form the corresponding metal hydroxides, which would affect the accuracy to some extent. It was found that the absorbance ratio reached the maximum value at alkaline media upon addition of Cd^{2+}. Since the pH value of the as-prepared ANS-AgNPs was 9.8, to save the time and cost, the original solution (pH around 9.8), which was the condition of the as-prepared ANS-AgNPs without any pH adjustments, was selected.

To estimate the kinetics on the aggregation of ANS-AgNPs induced by Cd^{2+}, we studied the time-dependent A_{580nm}/A_{390nm} values from the UV–Vis absorption spectra of ANS-AgNPs in the presence of Cd^{2+} at different times from 0 to 10 min. As shown in Fig. S7B, the absorbance ratio increased very rapidly within 3 min and then changed subtly, and the equilibrium was achieved in 5 min. Therefore, 5 min was chosen as the reaction time in the following tests for Cd^{2+}.

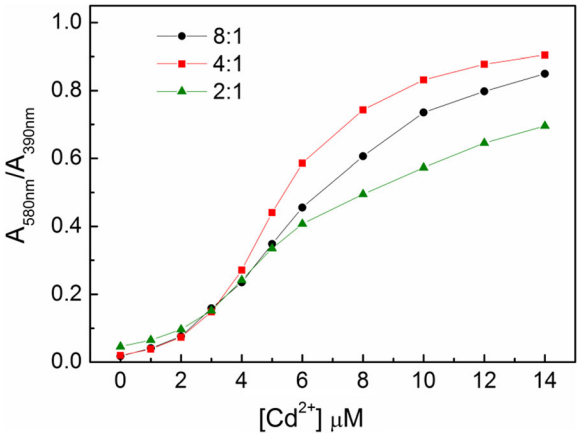

Fig. 3 Influence of the concentration of ANS on the absorbance ratio (A_{580nm}/A_{390nm}) of ANS-AgNPs

Sensitivity of the colorimetric assay for Cd^{2+}

In order to evaluate the sensitivity of the developed colorimetric method, under the above optimized conditions, the absorption spectra of ANS-AgNPs to different concentrations of Cd^{2+} were recorded. As the concentration of Cd^{2+} increased, the UV–Vis absorbance curves showed a red shift and broadened gradually and a new absorption peak emerged slowly at a longer wavelength (580 nm). Furthermore, with the increase of the concentration of Cd^{2+}, the color of the ANS-AgNPs gradually changes from yellow to orange and finally to reddish-brown (Fig. 4), suggesting the Cd^{2+} concentration-dependent aggregation of ANS-AgNPs. For quantitative analysis of Cd^{2+}, the absorbance ratio at 580 and 390 nm was used. A linear correlation existed between A_{580nm}/A_{390nm} and the Cd^{2+} concentration in the range from 1.0 to 10 μM (as shown in the inset in Fig. 4). The calibration equation obtained was $y = 0.0987$ [C]/μM + 0.0159 with a correlation coefficient (R) of 0.997, where y is the absorbance ratio

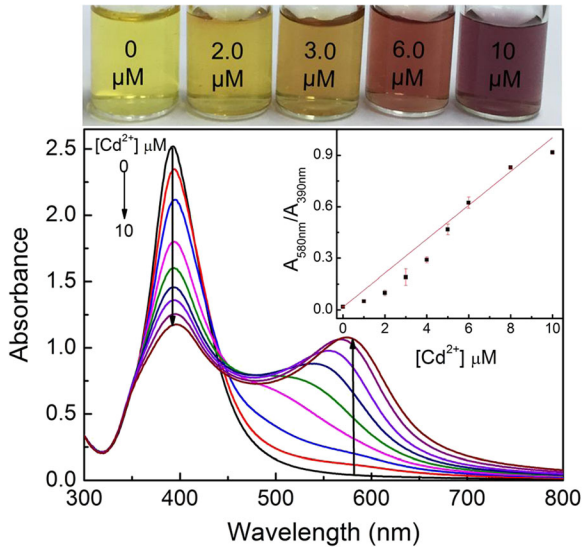

Fig. 4 Photographs and UV-visible spectra of ANS-AgNP solutions with various concentrations of Cd^{2+} in the range from 0 to 10 μM. *Inset* is the linear calibration curve between absorbance ratio A_{580nm}/A_{390nm} and the concentrations of Cd^{2+}

A_{580nm}/A_{390nm} and [C] is the concentration of Cd^{2+}. The limit of detection (LOD) was calculated to be 87 nM defined by the equation LOD = 3 S_0 / k, where S_0 is the standard deviation of blank measurements (n = 10) and k is the slope of the calibration curve. Compared with existing reported colorimetric methods of Cd^{2+}, our assay gave comparable detection limits (Table S1).

We also investigated the response of ANS-AuNPs to Cd^{2+}. Unlike that of ANS-AgNPs, ANS-AuNPs were testified to be insensitive to Cd^{2+} (Fig. S8). For this result, we explained the following: on the one hand, it is because the AuNP solution is acidic (pH ~5.5), in which the sulfonic group of ANS was too difficult to be deprotonated to bind to the Au atom. However, in the case of ANS-AgNPs, the basic environment of the solution (pH ~9.8) is very favorable for the deprotonation of the sulfonic group leading to the strong binding to the Ag atom. On the other hand, the as-synthesized AuNPs were capped with the citrate, which, to some extent, would block the contact between the Au atom and ANS. While for ANS-AgNPs, the bared AgNPs were prepared by $NaBH_4$ reduction, which is easier to be directly modificated with ANS due to the absence of any other ligand.

The effect of coexisting components

In order to examine the specific detection of Cd^{2+} using ANS-AgNPs, we investigated the potentially interfering components which may exist in milk, serum, and lake water. As shown in Fig. 5, the presence of the following amounts of foreign species compared with the concentration of Cd^{2+} resulted in less than ±10 % error: 100 times of Ag^+ and Ba^{2+}; 50 times of Mg^{2+}; 40 times of K^+; 35 times of Ca^{2+}; 30 times of Cu^{2+}; 15 times of Fe^{3+}; 10 times of Zn^{2+}, Al^{3+}, and Cr^{3+}; 5 times of Na^+ and Ni^{2+}; 2 times of Hg^{2+}; 1.5 times of Mn^{2+}; and 1 time of Pb^{2+} and Co^{2+}. Meanwhile, the effect of surface-active agents was also inspected. The existence of 50 times nonionic surfactant (polyoxyethylene nonylphenol ether, OP emulsifier) and 10 times anionic surfactant (sodium dodecyl sulfate, SDS) did not interfere. However, 1 time of cationic surfactant (cetyl trimethyl ammonium bromide, CTAB) interfered with the determination of Cd^{2+}, indicating that ANS-AgNPs had a negative charge. These results showed that the present method had good anti-interfering ability toward Cd^{2+} against coexisting components.

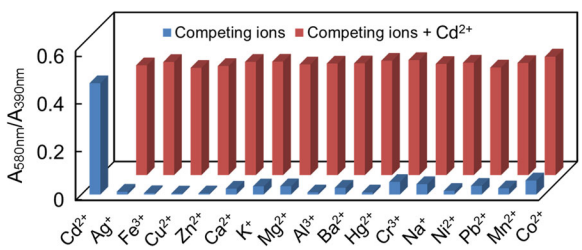

Fig. 5 Selectivity of the ANS-AgNPs for Cd^{2+} detection. *Blue bars* represent the absorbance ratio of ANS-AgNPs in the presence of Cd^{2+} or the competing ions. The concentrations of metal ions are all 5.0 μM. *Red bars* are the responses of ANS-AgNPs for a mixture of Cd^{2+} (5.0 μM) and maximum amounts of competing ions (color figure online)

Practical application

To evaluate the applicability of the colorimetric assay to real samples, lake water, milk powder, and serum were spiked with Cd^{2+} and tested in the assay. The detailed pretreatments of real samples were presented in Electronic Supplementary Materials. As summarized in Table 1, the mean recoveries of these samples are between 88.3 and 106 %. Such excellent results suggested that other chemical species present in samples did not interfere with the quantification of Cd^{2+}. These results clearly indicate that the proposed method is able to detect Cd^{2+} from various samples with high sensitivity and excellent selectivity.

Table 1 Determination of Cd^{2+} in real samples

Sample	Cd^{2+} added (μM)	Cd^{2+} found (μM)	Recovery (%)	RSD (%, n = 3)
Milk powder	0	Not found	–	–
	2.00	1.83 ± 0.20	91.6	10.7
	5.00	4.85 ± 0.44	96.9	9.06
	7.00	7.44 ± 0.66	106	8.84
Serum	0	Not found	–	–
	2.00	1.95 ± 0.11	97.3	5.84
	5.00	4.41 ± 0.23	88.3	5.29
	7.00	6.59 ± 0.08	94.2	1.27
Lake water	0	Not found	–	–
	2.00	1.91 ± 0.06	95.7	3.30
	5.00	4.87 ± 0.41	97.5	8.40
	7.00	7.27 ± 0.26	104	3.63

Conclusions

In this paper, a facile and rapid colorimetric method has been developed for the detection of Cd^{2+} using ANS-AgNPs as the colorimetric probe. The ANS-AgNPs showed specific recognition to Cd^{2+} accompanied by the color change from bright yellow to reddish-brown, which could be observed with the naked eye. It was demonstrated that the aggregation of ANS-AgNPs induced by Cd^{2+} was attributed to cooperative metal-ligand interaction between Cd^{2+} and ANS. The absorbance ratio A_{580nm}/A_{390nm} was linear with the concentration of Cd^{2+} ranging from 1.0 to 10 μM with a correlation coefficient of 0.997, and LOD was as low as 87 nM. Finally, this developed method was successfully applied to determinate Cd^{2+} in milk powder, serum, and lake water with satisfactory results. Therefore, this assay opens up new possibilities for developing analytical methods using ANS-AgNPs as a colorimetric probe for the monitoring of Cd^{2+} in real samples.

Acknowledgments The first two authors contributed equally to this work. This work is financially supported by the Natural Science Foundation of China (Nos. 21365014, 21505067) and Jiangxi ProvinceScience and Technology University Ground Plan project (KJLD No. 14007).

References

Akesson A, Julin B, Wolk A (2008) Long-term dietary cadmium intake and postmenopausal endometrial cancer incidence: a population-based prospective cohort study. Cancer Res 68: 6435–6441

Chansuvarn W, Tuntulani T, Imyim A (2015) Colorimetric detection of mercury(II) based on gold nanoparticles, fluorescent gold nanoclusters and other gold-based nanomaterials. Trends in Anal Chem 65:83–96

Chen WW, Cao FJ, Zheng WS, Tian Y, Xian YL, Xu P, Zhang W, Wang Z, Deng K, Jiang XY (2015a) Detection of the nanomolar level of total Cr[(III) and (VI)] by functionalized gold nanoparticles and a smartphone with the assistance of theoretical calculation models. Nanoscale 7:2042–2049

Chen HM, Hu WH, Li CM (2015b) Colorimetric detection of mercury(II) based on 2,2′-bipyridyl induced quasi-linear aggregation of gold nanoparticles. Sensors Actuators B Chem 215:421–427

Daher RT (1995) Trace metals (lead and cadmium exposure screening). Anal Chem 67:405R–410R

Darwish IA, Blake DA (2001) One-step competitive immunoassay for cadmium ions: development and validation for environmental water samples. Anal Chem 73:1889–1895

Davis AC, Wu P, Zhang XF, Hou XD, Jones BT (2006) Determination of cadmium in biological sample. Appl Spectrosc 41:35–75

Dobson S (1992) Cadmium: environmental aspects. World Health Organization, Geneva

Friberg L, Elinder CG, Kjellstrom T (1992) Cadmium. World Health Organization, Geneva

Guo W, Hu SH, Xiao YF, Zhang HF, Xie XJ (2010) Direct determination of trace cadmium in envirinmental samples by dynamic reaction cell inductively coupled plasma mass spectrometry. Chemosphere 81:1463–1468

Guo YG, Zhang Y, Shao HW, Wang Z, Wang XF, Jiang XF (2014) Label-free colorimetric detection of cadmium ions in rice samples using gold nanoparticles. Anal Chem 86:8530–8534

Jaliehvand F, Leung BO, Mah V (2009) Cadmium(II) complex formation with cysteine and penicillamine. Inorg Chem 48: 5758–5771

Jane AM, Matin MS, Amy T, John MH, Polly AN (2006) Cadmium exposure and breast cancer risk. J Natl Cancer Inst 98:869–873

Kumar VV, Anthony SP (2014) Silver nanoparticles based selective colorimetric sensor for Cd^{2+}, Hg^{2+}, and Pb^{2+} ions: tuning sensitivity and selectivity using co-stabilizing agents. Sensors Actuators B Chem 191:31–36

Li HB, Li FY, Han CP, Cui ZM, Xie GY, Zhang AQ (2010) Highly sensitive and selective tryptophan colorimetric sensor based on 4,4-bipyridine-functionalized silver nanoparticles. Sensors Actuators B Chem 145:194–199

Manjumeena R, Duraibabu D, Rajamuthuramalingam T, Venkatesan R, Kalaichelvan PT (2015) Highly responsive glutathione functionalized green AuNPs probe for precise colorimetric detection of Cd^{2+} contamination in the environment. RSC Adv 5:69124–69133

Martinez RH, Blasco IN (2012) Estimation of dietary intake and content of lead and cadmium in infant cereals marketed in Spain. Food Control 26:6–14

Matsumoto A, Osaki S, Kobata T, Hashimoto B, Uchihara H, Nakahara T (2010) Determination of cadmium by an improved double chamber electrothermal vaporization inductively coupled plasma atomic emission spectrometry. Microchem J 95:85–89

McLaughlin MJS, Singh BR (1999) Cadmium in soils and plants. Kluwer, Dordrecht

Medley CD, Smith JE, Tang ZW, Wu YR, Bamrungsap S, Tan WH (2008) Gold nanoparticle-based colorimetric assay for the direct detection of cancerous cells. Anal Chem 80:1067–1072

Mehta VN, Singhal RK, Kailasa SK (2015) A molecular assembly of piperidine carboxylic acid dithiocarbamate on gold nanoparticles for the selective and sensitive detection of Al^{3+} ion in water samples. RSC Adv 5:33468–33477

Mirabi A, Dalirandeh Z, Rad AS (2015) Preparation of modified magnetic nanoparticles as a sorbent for the preconcentration and determination of cadmium ions in food and environmental water samples pripr to flame atomic absorption spectrometry. J Magn Magn Mater 381:138–144

Ratnarathron N, Chailapakul O, Dungchai W (2015) Highly sensitive colorimetric detection of lead using maleic acid functionalized gold nanoparticles. Talanta 132:613–618

Sharif T, Niaz A, Najeeb M, Zaman MI, Ihsan M, Sirajuddin (2015) Isonicotinic acid hydrazide-based silver nanoparticles

as simple colorimetric sensor for the detection of Cr^{3+}. Sensors Actuators B Chem 216:402–408

Wan Z, Xu ZR, Wang JH (2006) Flow injection on-line solid phase extraction for ultra-trace lead screening with hydride generation atomic fluorescence spectrometry. Analyst 131:141–147

Willemse CM, Tlhomelang K, Jahed N, Baker PG, Iwuoha EI (2011) Metallo-graphene nanocomposite electrocatalytic platform for the determination of toxic metal ions. Sensors 11:3970–3987

Xue Y, Zhao H, Wu ZJ, Li XJ, He YJ, Yuan ZB (2011) Colorimetric of Cd^{2+} using gold nanoparticles cofunctionalized with 6-mercaotonicotinic acid and L-cysteine. Analyst 136:3725–3730

Yang NN, Gao YX, Zhang YJ, Shen ZY, Wu AG (2014) A new rapid colorimetric detection method of Al^{3+} with high sensitivity and excellent selectivity based on a new mechanism of aggregation of smaller etched silver nanoparticles. Talanta 122:272–277

Yunus S, Charles S, Dubois F, Vander Donckt E (2008) Simultaneous determination of cadmium(II) and zinc(II) by molecular fluorescence spectroscopy and multiple linear regression using an anthrylpentaazamacrocycle chemosensor. J Fluoresc 18:499–506

Zhan SS, Xu HC, Zhan XJ, Wu YG, Wang LM, Lv J, Zhou P (2015) Determination of silver(I) ion based on the aggregation of gold nanoparticles caused by silver-specific DNA, and its effect on the fluorescence of rhodamine B. Microchim Acta 182:1411–1419

Zhang M, Ye BC (2011) Colorimetric chiral recognition of enantiomers using the nucleotide-capped silver nanoparticles. Anal Chem 83:1504–1509

Zhang M, Liu YQ, Ye BC (2012) Colorimetric assay for parallel detection of Cd^{2+}, Ni^{2+}, and Co^{2+} using peptide-modified gold nanoparticles. Analyst 137:601–607